

# Multiple scattering and PXR: kinematical suppression of multiple scattering influence on PXR and dynamical shift of diffraction peaks

Konstantin Batrakov

*Institute for Nuclear Problems, Belarus State University.*

## Abstract

One feature of passing relativistic electron through a single crystal is emission of parametric X-ray radiation (PXR) due to diffraction on a crystallographic planes. As was shown in [1], PXR and coherent bremsstrahlung (CBS) take place for non-relativistic (or slow relativistic) electrons too. In this case emission spectrum consists of number of peaks corresponding to crystal reflexes in background of incoherent bremsstrahlung. These peaks are distinguished only for thin crystals, because the influence of electron multiple scattering on radiation increases with the crystal thickness and, as a result, smoothes out peaks. Simulation of PXR and CBS emission and considering of multiple scattering influence on spectra are carried out in present work. The optimal geometry with suppressed influence of multiple scattering is considered. Optimal geometry corresponds to the following condition

$$\cos \psi = 1 / \sqrt{1 + \left( \frac{\beta_u \sin \theta}{1 - \beta_u \cos \theta} \right)^2}.$$

Here  $\psi$  is inclination angle of electron velocity vector relative to the reciprocal lattice vector corresponding to the reflex under consideration.  $\beta_u = u/c$ , where  $u$  is average velocity of electron in beam,  $\theta$  is the angle between velocity and wave vector of emitted photon. Optimal geometry gives possibility to use more thick crystals for PXR generation. The dynamical shift of PXR peaks which is one more feature of multiple scattering influence is predicted and discussed.

## I. INTRODUCTION

PXR is the radiation from a charged particle due to the photon diffraction on the planes of a single crystal. It was shown both theoretically and experimentally and citation therein) that PXR from a relativistic electron ( $E \geq 50$  MeV) led to very high spectral intensity within the narrow angular and spectral range ( $\Delta\theta \sim \Delta\omega/\omega \sim 10^{-3}$ ).

Work [1] discussed and explained diffraction peaks produced experimentally in [2, 3, 4] for non-relativistic electrons ( $E \sim 50 \div 100$  keV) on the basis of interference between PXR and CBS. But the non-relativistic electron beam passing through the crystal is under the strong action of Coulomb multiple scattering. Its action is so great that the electron beam becomes completely isotropic after passing through the crystal with the thickness of order of several microns. So, the PXR and CBS is lost in the background of incoherent bremsstrahlung. For observation of PXR and CBS peaks the crystal must be sufficiently thin ( $\sim 0.1 \mu\text{m}$ ).

In the present paper influence of multiple scattering on PXR and CBS peaks is studied. The features of PXR and CBS such as dynamical peak frequency shifts and kinematical suppression of multiple scattering are derived and discussed.

## II. ACCOUNT OF MULTIPLE SCATTERING

Corresponding to Feranchuk [1], the spectral-angular distribution of emitted quanta has form:

$$d^2N_{\mathbf{n}\omega}^{(s)} = \frac{e^2\omega}{4\pi\hbar c^3} \sum_{\mathbf{g}} \left| \mathbf{v}_0 \mathbf{E}_{g_s} - \frac{e}{m} \frac{\mathbf{e}_s \mathbf{g}}{\mathbf{g} \mathbf{v}_0} U_g - \frac{e}{m} \mathbf{v}_0 \frac{\mathbf{k} \mathbf{g}}{(\mathbf{g} \mathbf{v}_0)^2} U_g \right|^2 \times \left| \frac{\exp[i((\mathbf{k} + \mathbf{g}) \mathbf{v}_0 - \omega)t] - 1}{(\mathbf{k} + \mathbf{g}) \mathbf{v}_0 - \omega} \right|^2 d\omega d\Omega. \quad (1)$$

Here  $\mathbf{E}_{g_s} = \chi_g (c^2 \mathbf{k}_g (\mathbf{g} \mathbf{e}_s) - \omega^2 \mathbf{e}_s) / (k_g^2 c^2 - \omega^2)$ ,  $U_g = \chi_g$  is crystal polarizabilities,  $\mathbf{e}_s$  is photon polarization vector,  $\mathbf{g}$  is reciprocal lattice vector,  $\mathbf{v}_0$  is electron velocity,  $e, m$  are electron electrical charge and mass.  $t$  is time of electron passing through the crystal,  $\mathbf{k}$  and  $\omega$  are wave vector and frequency of emitted photons.

Electron beam under action of multiple scattering acquires velocity spread, therefore (1)

should be averaged over this spread:

$$d^2 N_{\mathbf{n}\omega}^{(s)} = \frac{e^2 \omega}{4\pi \hbar c^3} \int \frac{d\varphi_0}{2\pi} d\theta_0 \theta_0 f(\theta_0) \sum_{\mathbf{g}} \left| \mathbf{v}_0 \mathbf{E}_{g_s} - \frac{e}{m} \frac{\mathbf{e}_s \mathbf{g}}{\mathbf{g} \mathbf{v}_0} U_g - \frac{e}{m} \mathbf{v}_0 \frac{\mathbf{k} \mathbf{g}}{(\mathbf{g} \mathbf{v}_0)^2} U_g \right|^2 \times \left| \frac{\exp[i((\mathbf{k} + \mathbf{g}) \mathbf{v}_0 - \omega)t] - 1}{(\mathbf{k} + \mathbf{g}) \mathbf{v}_0 - \omega} \right|^2 d\omega d\Omega. \quad (2)$$

In (2)  $f(\theta_0)$  is distribution function of electron beam ( $\theta_0$  is angle relative to vector of average velocity). Distribution function will be used in gaussian form

$$f(\theta_0) = \frac{2 \exp \left\{ -\frac{\theta_0^2}{\theta_s^2} \right\}}{\theta_s^2}. \quad (3)$$

In (3)  $\theta_s$  is scattering angle the square of which equals to  $\theta_s^2 = 16\pi n_0 Z(Z + 1) r_e^2 \frac{(E + 1)^2}{E^2 (E + 2)^2} L_K L_e$ .  $L_e$  is an electron path in crystal [5],  $Z$  is the crystal atom number,  $E = T/(mc^2)$ ,  $T$  is electron kinetic energy,  $L_k$  is Coulomb logarithm,  $n_0$  is atom density. Typical value of scattering angle for *Si* at path length 1  $\mu\text{m}$  is  $\theta_s \sim 0.4$  rad. In (2) angular dispersion is taken into account only. Energy dispersion and energy losses exerts significantly less influence on radiation at considered energies (electron energy losses on ionization in *Si* is of order of 100 eV at electron energy  $E = 100$  keV and crystal thickness 1  $\mu\text{m}$ ).

Line width of electron spontaneous emission without accounting the multiple scattering can be estimated as  $\Delta\omega/\omega \sim 1/(kL_e)$  (if  $L_e$  is less than absorption length) and it gives  $\Delta\omega/\omega \sim 10^{-2}$  for crystal thickness  $\sim 0.1$   $\mu\text{m}$ . Therefore, scattering angle for crystal  $\geq 0.1$   $\mu\text{m}$  is greater than spontaneous emission line width. In this case we can use in (2) the following approximation

$$\left| \frac{\exp[i((\mathbf{k} + \mathbf{g}) \mathbf{v}_0 - \omega)t] - 1}{(\mathbf{k} + \mathbf{g}) \mathbf{v}_0 - \omega} \right|^2 = 2\pi \delta(\omega - (\mathbf{k} + \mathbf{g}) \mathbf{v}_0) \frac{1 - \exp\{-k_z'' L\}}{k_z'' v_{0z}}, \quad (4)$$

where  $k_z''$  is imaginary part of wave vector component  $k_z$ ,  $L$  is crystal thickness. Integrating

(2) over  $\theta_0$  gives

$$\begin{aligned}
d^2 N_{\vec{n}\omega}^{(s)} &= \frac{e^2 1 - \exp\{-k_z'' L\}}{4\pi \hbar c^3 k_z'' u_z \pi \theta_s^2} \sum_{\vec{g}} |A|^2 \int' d\varphi_0 \frac{1}{\sqrt{[\tan(\theta_g) \cos(\varphi - \varphi_0)]^2 - 2\Delta_g}} \times \\
&\quad \times \left\{ \left( \tan(\theta_g) \cos(\varphi - \varphi_0) + \sqrt{[\tan(\theta_g) \cos(\varphi - \varphi_0)]^2 - 2\Delta_g} \right) \right. \\
&\quad \exp \left[ - \left( \tan(\theta_g) \cos(\varphi - \varphi_0) + \sqrt{[\tan(\theta_g) \cos(\varphi - \varphi_0)]^2 - 2\Delta_g} \right)^2 / \theta_s^2 \right] + \\
&\quad \left. + \left( \tan(\theta_g) \cos(\varphi - \varphi_0) - \sqrt{[\tan(\theta_g) \cos(\varphi - \varphi_0)]^2 - 2\Delta_g} \right) \right. \\
&\quad \left. \exp \left[ - \left( \tan(\theta_g) \cos(\varphi - \varphi_0) - \sqrt{[\tan(\theta_g) \cos(\varphi - \varphi_0)]^2 - 2\Delta_g} \right)^2 / \theta_s^2 \right] \right\} d\omega \Omega.
\end{aligned} \tag{5}$$

Here  $\varphi, \varphi_0$  are the polar angles corresponding to wave vector and electron velocity vector.  $\theta_g$  is angle between vector  $\mathbf{k} + \mathbf{g}$  and average velocity vector  $\mathbf{v}_0$ .  $\Delta_g = (\omega - (\mathbf{k} + \mathbf{g})\mathbf{v}_0) / \omega$  is parameter of detuning from synchronism. The prime over the integral means that integration of terms containing  $z_1 = \tan(\theta_g) \cos(\varphi - \varphi_0) + \sqrt{[\tan(\theta_g) \cos(\varphi - \varphi_0)]^2 - 2\Delta_g}$  and  $z_2 = \tan(\theta_g) \cos(\varphi - \varphi_0) - \sqrt{[\tan(\theta_g) \cos(\varphi - \varphi_0)]^2 - 2\Delta_g}$  is fulfilled in regions of  $\varphi_0$ , where  $z_1$  and  $z_2$  are positive. For convenience let's perform substitution  $x = \cos(\varphi - \varphi_0)$ . That gives the integral in the form

$$\begin{aligned}
&2 \int' \frac{dx}{\pi \theta_s^2 \sqrt{[\tan(\theta_g)x]^2 - 2\Delta_g} \sqrt{1-x^2}} \\
&\left\{ \left( \tan(\theta_g)x + \sqrt{[\tan(\theta_g)x]^2 - 2\Delta_g} \right) \exp \left[ - \left( \tan(\theta_g)x + \sqrt{\tan^2(\theta_g)x^2 - 2\Delta_g} \right)^2 / \theta_s^2 \right] + \right. \\
&\left. \left( \tan(\theta_g)x - \sqrt{[\tan(\theta_g)x]^2 - 2\Delta_g} \right) \exp \left[ - \left( \tan(\theta_g)x - \sqrt{\tan^2(\theta_g)x^2 - 2\Delta_g} \right)^2 / \theta_s^2 \right] \right\}.
\end{aligned} \tag{6}$$

In (6) integration is fulfilled over the regions of  $-1 \dots 1$ , in which  $z_1$  and  $z_2$  are positive. As was mentioned above even for crystal thickness  $L \sim 0.1 \mu\text{m}$  scattering angle exceeds spontaneous emission line width  $\theta_s > 1/(kL_e)$ . As a result, emission line is widened and spectral-angular brightness reduces. It is very desirable to decrease the influence of multiple scattering. Such possibility really exists. So  $\mathbf{k}_g \mathbf{v}_0 = k_g v_0 \cos(\theta_g)$ , then due to electron beam spreading  $\cos(\theta_g + \theta_s) \approx \cos(\theta_g) - \sin(\theta_g)\theta_s - \cos(\theta_g)\theta_s^2/2$ . Therefore if  $\sin(\theta_g) = 0$ , the terms corresponding to detuning from synchronism ( $\omega - \mathbf{k}_g \mathbf{v}_0 \approx 0$ ) are proportional to  $\theta_s^2$ , not to  $\theta_s$ . So, when  $\theta_s \ll 1$ , the geometry with  $\sin \theta_g = 0$  is preferable. As will be shown bellow in section III this geometry actually can essentially increase (on several orders) spectral-angular

brightness of emission.

Corresponding to (4) the emission peaks of single electron has frequencies

$$\omega_g = \frac{\mathbf{g}\mathbf{v}_0}{1 - \mathbf{n}\mathbf{v}_0/c}. \quad (7)$$

Here  $\mathbf{n}$  is a unit vector having direction of wave vector. So, position of these peaks depends on reciprocal vector  $\mathbf{g}$  and on angle of photon observation. Therefore, spectral distribution measured by detector at fixed angle is looked as the set of peaks on the background of incoherent bremsstrahlung. The peaks position changes as with the observation angle change so with crystal rotation. Therefore, emission spectrum is easy tuned. Due to multiple scattering electron beam acquires velocity spread, which leads to frequency spread in correspondence to expression (7). First term of (1) corresponding to PXR depends on polarizability  $\chi_g$ .  $|\chi_g|^2 \sim \omega^{-4}$ , therefore this term increases with frequency decrease. On the other hand, CBS grows with frequency increase. Therefore, if PXR exceeds CBS, then diffraction peak drift in soft spectral range. On the contrary, if CBS essentially exceeds PXR then diffraction peak shifts in region with larger frequency. This dynamical frequency shift will be demonstrated in III.

### III. DISCUSSION AND ESTIMATIONS.

Let's study some common features of spectral angular distribution accounting the multiple scattering. If  $\tan \theta_g \geq 1$ , then following estimation of (6) can be made

$$\frac{2}{\theta_s^2} \exp \left\{ -\frac{2 \tan^2(\theta_g)}{\theta_s^2} \right\} \text{I}_0 \left( \frac{2 \tan^2(\theta_g)}{\theta_s^2} \right) + \frac{1}{\sqrt{\pi} \tan(\theta_g) \theta_s} \exp \left\{ -\frac{\Delta_g^2}{\tan^2(\theta_g) \theta_s^2} \right\}. \quad (8)$$

Expression (8) is true if  $\tan(\theta_g) \gg \Delta_g$  and  $\tan(\theta_g) \gg \theta_s$ . The first term of (8) is proportional  $h = \exp \left\{ -\frac{2 \tan^2(\theta_g)}{\theta_s^2} \right\} \text{I}_0 \left( \frac{2 \tan^2(\theta_g)}{\theta_s^2} \right)$  (dependence  $h(z)$  on its argument is shown on Fig. 1a). It follows that spectral width of diffraction peak  $\delta\omega/\omega$  is proportional to  $|\tan(\theta_g)|\theta_s$  and maximal brightness grows with reducing this width. So, spectral brightness increases with decreasing  $|\tan(\theta_g)|$  as was predicted in II and kinematical suppressing of multiple scattering influence takes place.

In opposite case  $|\tan(\theta_g)| = 0$  (6) can be estimated as

$$\frac{2 \exp \left\{ -\frac{2|\Delta_g|}{\theta_s^2} \right\}}{\theta_s^2}, \quad (9)$$

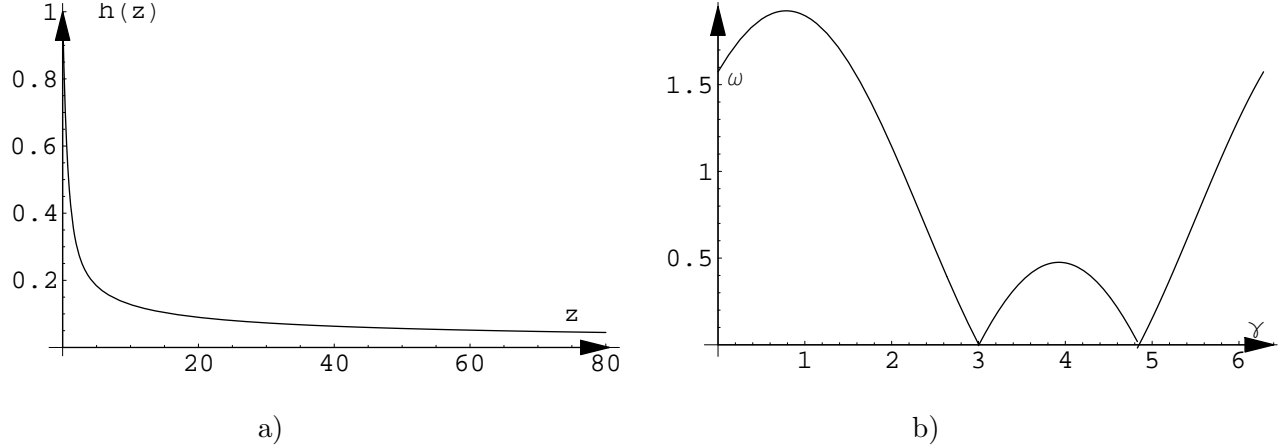


FIG. 1: a) Graphic of function  $h(z)$  dependence on its argument; b) Frequency dependence on  $\gamma$ . Si [0 0 1], reflex (1 1 1). Electron energy  $E = 75$  KeV.

and spectral width  $\delta\omega/\omega$  is proportional to scattering angle squared. Expression (9) is true for  $\Delta_g \gg \tan\theta_g$ . (9) is applied for large angle  $\theta_g$  also. It follows from (8) and (9) that when  $\mathbf{k} + \mathbf{g} \parallel \mathbf{v}$ , value of spectral intensity exceeds the spectral intensity for  $\tan\theta_g \gg \theta_s$  in  $\sim \tan\theta_g/\theta_s$  times. When using crystal with thickness for which  $\theta_s \gg 1$  it is generated bright and narrow spectral line.

Let us study frequency dependence of diffraction peaks on crystal rotation angles. Rotation will be described by standard Euler angles  $\alpha, \beta, \gamma$  between normal to the crystal surface and velocity vector (which is parallel to  $Z$  axis). Here  $\alpha$  changing in the range  $0 \dots 2\pi$  is the rotation angle relative to vector  $v$ ,  $\beta$  changing in range  $0 \dots \pi$  is rotation angle relative to new axis (1 0 0) and  $\gamma$  changing in the range  $0 \dots 2\pi$  is the rotation angle relative to the new  $Z'$  axis. It is evident that peak frequency can't depend on  $\alpha$  because independence of scalar product  $\mathbf{g}\mathbf{v}$  on  $\alpha$ . Dependence of frequency on  $\gamma$  and  $\beta$  is shown on Figs. 1b and 2a.

It can be seen from figures that frequency changes in wide spectral range due to crystal rotation. Frequency changes with change of observation angle also. This is shown on Fig. 2b. These figures of frequency dependence were built with the help of the formula

$$\omega = \frac{2\pi\beta_u n_3 \cos\beta + n_2 \sin\beta \cos\gamma + n_1 \sin\beta \sin\gamma}{a(1 - \beta_u \cos\theta)}, \quad (10)$$

which follows from (7) if crystal surface coincides with crystallographic plane [0 0 1],  $\beta_u = v_0/c$ .  $n_1, n_2, n_3$  are indices corresponding to concerned reflexes.

Very effective demonstration of orientation dependence is splitting of reflexes frequencies. For example, all reflexes of crystal [1 1 1] with same sum  $k + l + m$  are degenerated at zero

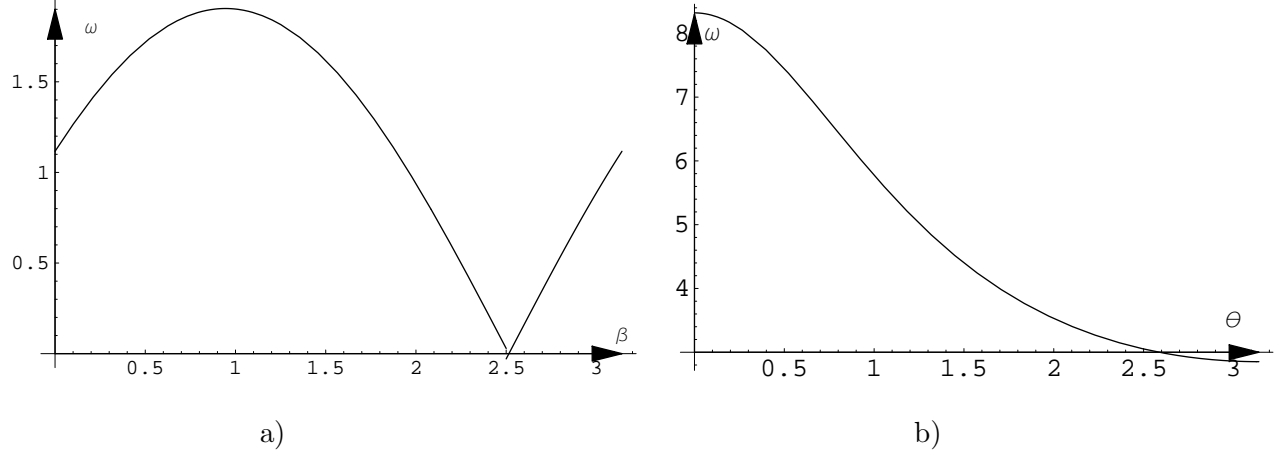


FIG. 2: a) Frequency dependence on  $\beta$ , Si [0 0 1], reflex (1 1 1). Electron energy  $E = 75$  KeV.; b) Frequency dependence on observation angle  $\theta$ , Si [0 0 1], reflex (0 0 4). Electron energy  $E = 75$  KeV.

angle of crystal inclination. This degeneration is disappeared if we incline crystal on angle  $\beta$ . Dependence of frequency on angle  $\gamma$  is shown on Figure 3. It is seen, that for the case when crystal is not inclined, frequencies for all reflexes with  $k + l + m = 7$  are the same and not change. But when crystal is inclined on  $\beta = 3$  degrees, reflexes split and their frequencies depend on  $\gamma$ . Let's note, that at different values of angle  $\gamma$  we shall see different number of reflexes frequencies.

As was shown in (8) and (9), brightness has maximal magnitude at  $\theta_g \approx 0$ . Let's study this geometry in more detail. It follows from (7) and requirement of  $\mathbf{k} + \mathbf{g} \parallel \mathbf{u}$  for  $\theta_g = 0$  the condition

$$\frac{\mathbf{g}\beta_u}{1 - \beta_u \mathbf{n}} \mathbf{n} + \mathbf{g} \parallel \beta_u \quad (11)$$

must be fulfilled. It follows from (11), that component of vector  $\mathbf{g}$  which is parallel to  $[\mathbf{k} \times \mathbf{u}]$  must be zero. Besides, component of vector in left hand side of (11) which is perpendicular to  $\mathbf{u}$  and lies in plane of  $\mathbf{k}$  and  $\mathbf{u}$  must be zero also. This leads to expression for  $\psi = \widehat{\mathbf{g}\mathbf{v}}$

$$\cos \psi = 1 / \sqrt{1 + \left( \frac{\beta_u \sin \theta}{1 - \beta_u \cos \theta} \right)^2}. \quad (12)$$

As it follows from (12), the parameters of optimal geometry depend on reflex, electron energy and observation angle. Specific observation angle corresponds to specific crystal rotation which gives maximal brightness for given reflex.

Dependence of  $\tan \theta_g$  on Euler angle  $\gamma$  is demonstrated on Figure 4. This graphic is built at fixed angles  $\alpha = 0, \beta = 1.1\pi/4, \theta = \pi/2 - 0.1$ . Angle between vector  $\mathbf{k} + \mathbf{g}$  and

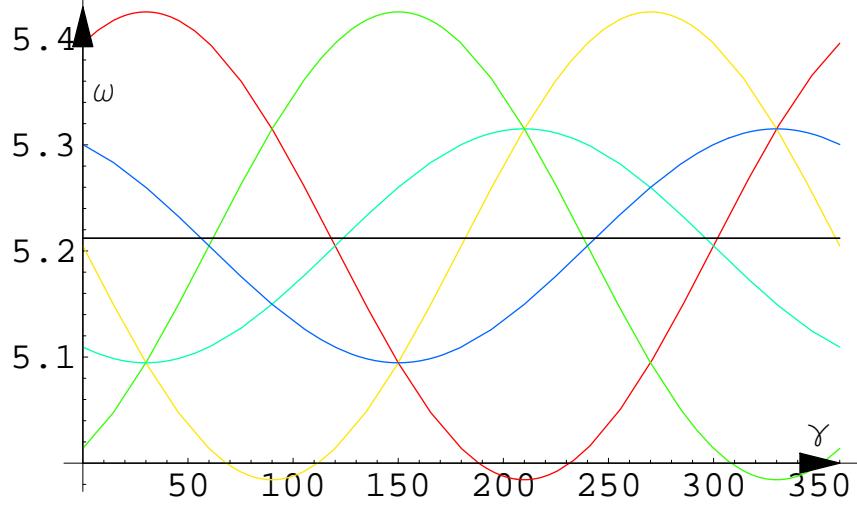


FIG. 3: Splitting of reflex  $k + l + m = 7$  (*Si* [1 1 1]) at nonzero  $\beta = 3^\circ$ ,  $E = 100$  KeV. Black line demonstrates dependence of peaks with  $k + l + m = 7$  on  $\gamma$  for zero inclination angle. Color curves show frequency dependence of reflexes (5 1 1), (1 1 5), (1 5 1), (1 3 3), (3 1 3), (3 3 1) on  $\gamma$  for inclination angle  $\beta = 3$  degrees.

electron velocity vector  $\mathbf{v}$   $\theta_g$  is in vicinity to zero when  $\gamma \approx 1.46$  for these parameters. It is evident that change of one angle parameter changes other angular parameters of target angular position and observation angle corresponding to  $\theta_g = 0$ .

Figure 5 corresponds to electron current  $1 \mu\text{A}$  and crystal thickness  $L \approx 0.1 \mu\text{m}$ . Other parameters is on the Figure It can be seen, that peak corresponding to optimal geometry is very bright and it width is about of 0.05 KeV. For comparison the dependence of spectral-angular brightness on frequency for non-optimal geometry is shown on Fig. 6. When the beam takes dispersion, then electrons which emit smaller frequencies will give greater contribution to emission due to increasing of polarizability at frequency reducing. So, peaks will shift in more soft region. On Fig. 6 point shows central frequency of diffraction peak without accounting of multiple scattering. Dynamical frequency shift corresponds to difference between these frequency. Such behavior of peak central frequency should be observed experimentally.

The brightness corresponding to optimal geometry (Fig. 5) exceeds in  $\sim 100$  times the brightness for non-optimal one (Fig. 6).

One more method to suppress multiple scattering influence on radiation is using of



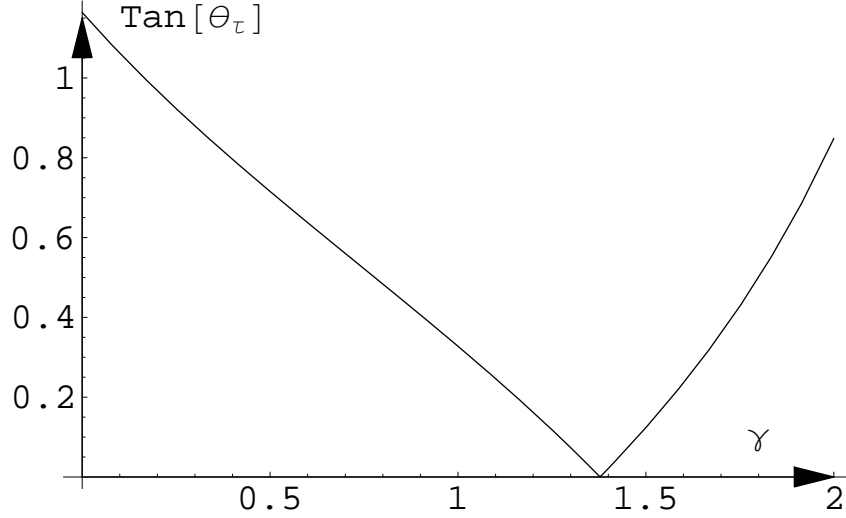


FIG. 4: Dependence of  $\tan \theta_g$  on Euler angle  $\gamma$ , Si [0 0 1], reflex (1 1 1). Electron energy  $E = 75$  KeV.

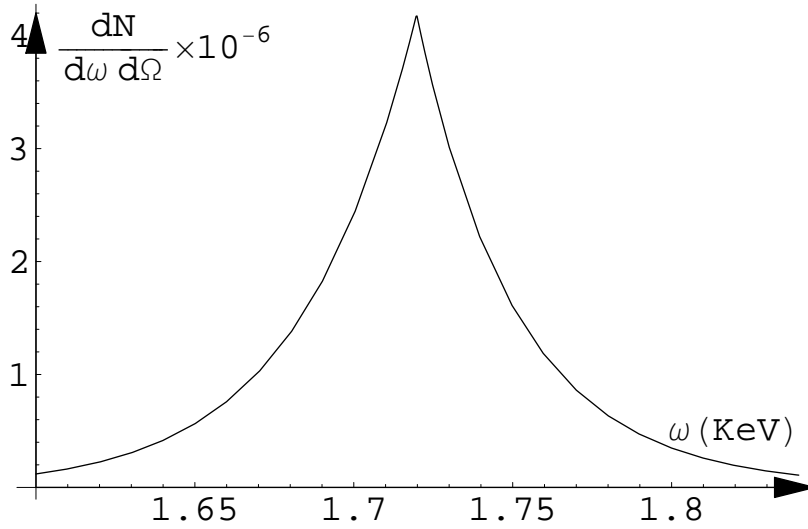


FIG. 5: Optimal geometry. Frequency dependence of emitted photon spectral angular density at  $\theta_g \approx 0$ .  $\gamma = 1.38$ ,  $\theta = \pi/2 - 0.1$ ,  $\alpha = 0$ ,  $\beta = 1.1\pi/4$ . Si [0 0 1], reflex (1 1 1), electron energy  $E = 75$  KeV.

inclined geometry geometry for PXR emitted photons observation. In the case when  $\psi_1/(k\chi_0'') \ll L$  ( $\psi_1$  is the angle between wave-vector  $\mathbf{k}$  and crystal surface), the emission will be detected from the electron which path is of order of  $\psi_1/(k\chi_0'')$ , not  $\sim L$  or  $\sim 1/(k\chi_0'')$ . If  $\psi_1/(k\chi_0'')$  is sufficiently small, emission from such path is not disturbed by multiple scatter-

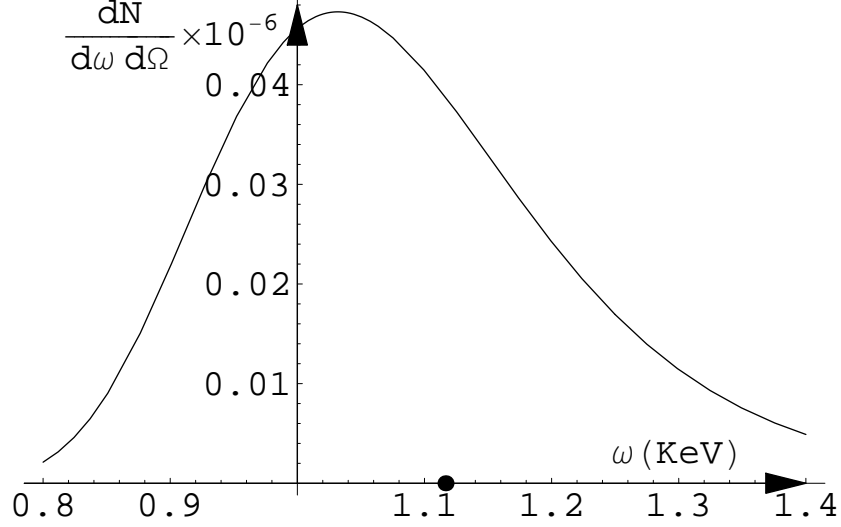


FIG. 6: Non-optimal geometry. Frequency dependence of emitted photon spectral angular density .  $\gamma = 0$ ,  $\theta = \pi/2 - 0.1$ ,  $\alpha = 0$ ,  $\beta = 0$ . Si [0 0 1], reflex (1 1 1), electron energy  $E = 75$  KeV. Point shows central frequency of diffraction peak without accounting of multiple scattering. Dynamical frequency shift corresponds to difference of this point frequency and real peak central frequency.

ing. Combining kinematical suppression with inclined observation geometry it is possible to produce very bright and narrow peak of PXR radiation.

#### IV. CONCLUSION

Regulation of multiple scattering action on PXR (CBS) emission by geometry choice gives possibility using relatively thick crystals for observation of diffraction peaks. Specific reflex and specific crystal orientation corresponds to specific observation angle and frequency where kinematical suppression is appeared. Therefore, experimental setup should have possibility of crystal target and detector orientation in wide spectral range.

## A. Acknowledgments

The work was fulfilled due to support ISTC: grant B-626.

---

- [1] I. D. Feranchuk, A. Ulyanenko, J. Harada and J. C. H. Spence, *Phys. Rev. A* **62**, 4225 (2000).
- [2] Y.S. Korobochko, V.F. Kosmach and V.I. Mineev, *Sov. Phys. JETP*, **21**, 834 (1965).
- [3] J.C.H. Spence and G. Reese, *Acta Crystallogr. A*, **42**, 577 (1986).
- [4] G.M. Reese, J.C.H. Spence and N. Yamamoto, *Philos. Mag. A*”, **49**, 697 (1984).
- [5] V.S. Remizovich, D. B. Rogozkin and M. I. Ryazanov, “Fluctuations of Free Path of Charged Particles”, *EnergoAtomIzdat, Moscow*, (1988).